Hindawi
International Journal of Photoenergy
Volume 2020, Article ID 6686797, 6 pages
https://doi.org/10.1155/2020/6686797

Research Article

Crystalline Silicon PERC Solar Cell with Ozonized AlOx Passivation Layer on the Rear Side

Pang-Kai Liu, Yu-Lun Cheng, and Likarn Wang

Institute of Photonics Technologies, National Tsing Hua University, Hsinchu, Taiwan

Correspondence should be addressed to Likarn Wang; lkwang@ee.nthu.edu.tw

Received 11 October 2020; Revised 6 November 2020; Accepted 25 November 2020; Published 4 December 2020

Academic Editor: Daniel T. Cotfas

Copyright © 2020 Pang-Kai Liu et al. This is an open access article distributed under the Creative Commons Attribution License, which permits unrestricted use, distribution, and reproduction in any medium, provided the original work is properly cited.

We present a method of ozonation to form the rear-side passivation layers of crystalline silicon PERC cells. In the method, a thin aluminum film was deposited on the back surface of a silicon wafer and then was oxidized into an aluminum oxide layer by gaseous ozone. Lifetimes of the wafers with such passivation layers proved to be increased with respect to those untreated, and the resultant PERC cells showed a performance improvement compared with standard cells with full back surface fields.

1. Introduction

A basic cell structure of crystalline silicon PERC (passivated emitter and rear cell) cells commonly fabricated by industry is shown in Figure 1 [1], where silver electrodes are screen printed on the front surface of a p-type textured wafer with an antireflection coating (ARC) and a diffused N+ layer, while local contacts are formed by fired aluminum paste at the laser-ablated parts of the back surface with a stack of AlOx/SiNx. A local BSF (back surface field) is formed on the rear contact to facilitate the collection of holes, and the thin AlOx (arising from Al_2O_3) layer contributing field-effect passivation will eject electrons and thus reduce recombination of electrons and holes near the rear side of the wafer [2].

The Al_2O_3 layer with an appropriate thickness can be deposited on a p-type silicon wafer by a PECVD [3, 4] or an ALD [5, 6] technique. The resultant passivation layer AlOx is formed at the interface of Si/Al_2O_3 after the wafer is annealed at a proper temperature and produces negative charges with a density that is several times as high as $10^{12}\,cm^{-2}$. In between silicon and AlOx, there exists a layer of SiOx in a tetrahedral geometry [7, 8]. The AlOx near the SiOx also has a tetrahedral geometry, rendering the insufficiency of aluminum atoms and henceforth negative charges. Nowadays, industrial PERC cells with such passivation layers have achieved a conversion efficiency of ~21% or even higher [9, 10]. Deposition of an Al_2O_3 layer by either PECVD or ALD, however, is not a cost-effective way because the precursor trimethylaluminum and a vacuum-processing facility are both required. Many different methods for the formation of Al_2O_3 layers for the purpose of passivation have been developed without using vacuum-chamber-equipped facilities.

A good passivation layer was obtained by using a technique of reactive sputtering without using trimethylaluminum, resulting in PERC cells that showed a significant improvement in efficiency compared with standard full BSF cells [11]. A printable aluminum oxide paste was demonstrated to support an efficiency of 20.1%, which could be easily integrated into an existing production line and cause a reduction of additional cost for equipment [12]. The researchers of [13] reported a high-level passivation with an Al_2O_3 layer synthesized on a p-type crystalline silicon wafer by a sol-gel method. The inventors of [14] proposed spraying methanol solution containing aluminum elements (or specifically, containing aluminum acetylacetonate) on the surface of a silicon wafer for forming a passivation layer. This idea could result in a tremendous reduction in manufacturing cost, however, leaving unsolved a problem of uneven thicknesses of the passivation layers from sample to sample. In this study, we present a different method for forming an Al_2O_3 layer for the back surface passivation of a PERC cell. Although vacuum-supported equipment is employed in the method, Al_2O_3 layers with a uniform thickness can be

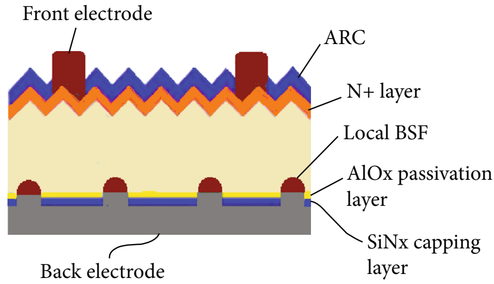

Figure 1: Structure of a crystalline silicon PERC cell commonly fabricated by industry.

formed without trimethylaluminum used. In this new method, a thin aluminum film was first deposited on the back surface of a phosphorus-diffused silicon wafer and then oxidized into an aluminum oxide layer by gaseous ozone. Such an aluminum oxide layer proved to produce a good level of passivation after annealed at a proper temperature. Section 2 reveals the formation of such a passivation layer and briefs the fabrication process of PERC cells in this study. Experimental results for minority carrier lifetime and cell performance measurements are presented in Section 3, followed by a conclusion section.

2. Experiments

2.1. Al_2O_3 Layer Formed by Ozonation Method. Pseudosquare- (100-) oriented 200 μm thick diamond-wire-sawn single-crystalline silicon wafers in the dimensions of $156 \times 156\,mm^2$ were cut into smaller pieces with a size of $5.2 \times 5.2\,cm^2$. For lifetime measurement, these wafers were treated to form an Al_2O_3 layer on, respectively, their front and back surfaces. To form the Al_2O_3 layer, we first used an e-gun evaporator to deposit a 3 nm thick aluminum film on the two surfaces of the wafer. The panel setting for this film thickness was 3 nm, which, however, was believed to be smaller than the true value of thickness, as we will see later. The as-deposited wafers were then put in a beaker with a piece of saran wrap covering its top for hermetic seal while allowing an ozone gas supplier to constantly feed the beaker with gaseous ozone. After a period of time, the aluminum films were transformed into Al_2O_3 films, followed then by an annealing process. Such a treatment for Al_2O_3 formation was also applied to commercial blue wafers as well as textured wafers, the latter of which had a surface morphology of inverted pyramid-like structure (see Figure 2) that was formed by using our proprietary method. Here, the commercial blue wafers refer to the wafers processed in an industrial production line up to the step of deposition of PECVD ARC layers. Al_2O_3 films were formed only on the back surfaces of these wafers, and so we could observe the improvement in lifetime with respect to untreated commercial blue wafers.

Figure 3 shows the stack of $Al_2O_3/SiO_2/Si$ for a sample that was originally coated with an aluminum film and was subsequently ozone-treated and annealed at 600°C for 90 seconds. It can be seen that the thicknesses of Al_2O_3 and SiO_2 read, respectively, 7.64 nm and 3.15 nm. In the following, we will show that this annealing condition gave rise to the best passivation effect. After oxidized, a 3 nm thick aluminum layer was supposed to become about 5 nm thick. The Al_2O_3 thickness obtained was not consistent with the expected for the possible reason of unreliable aluminum thickness at only several nanometers achieved by using e-gun evaporation.

A depth profile showing atomic compositions obtained by X-ray photoelectron spectroscopy is given in Figure 4 for a sample with the stack of $Al_2O_3/SiO_2/Si$ on a silicon substrate after the ozonation method was applied on the aluminum metal film, and the sample was annealed at 600°C for 90 seconds. Obviously, Al_2O_3 was formed at etch time less than ~100 seconds. After the etch time of 100 seconds, AlOx with $x > 1.5$ can be seen. For example, at the etch times between 125 and 150 seconds, x is about 1.7. However, we are aware that the depth profile does not appear to be as steep as it should be to show the respective layers on the silicon substrate. This is because the atomic composition at each etch time is taken as an average quantity over the atomic compositions obtained at neighboring etch times for the XPS instrument we used here. On the other hand, EDS analysis (Figure 5) reveals the compositions of Si, Al, O, and Pt (platinum) atoms, where Pt atoms were detected because the sample was covered with platinum metal for measurement. The oxygen/Si ratio appeared to be about 2 : 1 at the positions of 40-43 nm, indicating a layer of SiO_2 there. For the region of 43-45 nm, the oxide was much like SiO_4, indicating a tetrahedral geometry. Then away from the SiO_4 layer, i.e., from the position of ~45 nm, the number of Al atoms increased and supported the existence of AlOx, where $5 > x > 1.6$, with Al vacancy at the positions of 44-46 nm, and approach Al_2O_3 at farther positions, i.e., the positions of 46-53 nm. After the point of 53 nm, a rapidly growing number of Pt atoms were detected. The structural transition from SiOx to Al_2O_3 over the interface region was consistent with the remark in [7].

2.2. PERC Cell Fabrication. Here, we used diamond-wire-sawn single-crystalline silicon wafers for the study of PERC cells. These wafers were textured to have an inverted-pyramid-like structure on two sides and were then phosphorus diffused to form an n layer on the front side. After an Al_2O_3 layer was formed on the rear side of each diffused wafer with the size of $5.2 \times 5.2\,cm^2$, followed by annealing at 600°C for 90 seconds. Such an annealing condition was found to achieve the best minority carrier lifetime for bare wafers that were coated with Al_2O_3 on both sides and for diffused wafers coated with SiNx ARC on the front side and Al_2O_3 on the back side. Then, a 100 nm thick SiNx layer was deposited on the Al_2O_3 layer by PECVD, resulting in a stack of Al_2O_3/SiNx on the rear side. A photolithographic process was subsequently employed to form a pattern of line-shaped openings on the rear side. Then, a SiNx layer with a thickness of 100 nm was deposited by PECVD to form an ARC layer on the front side. Aluminum paste and silver paste were subsequently screen printed on the rear side and the front side, respectively, followed by cofiring in a conveyor belt furnace.

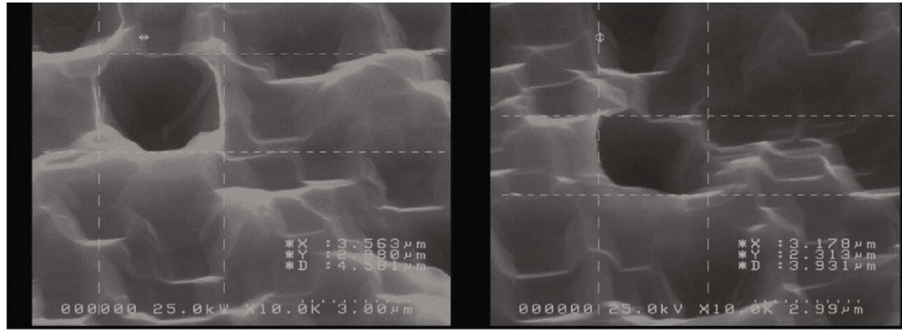

FIGURE 2: Surface morphologies measured at two positions of the wafer used for PERC cell fabrication in the study.

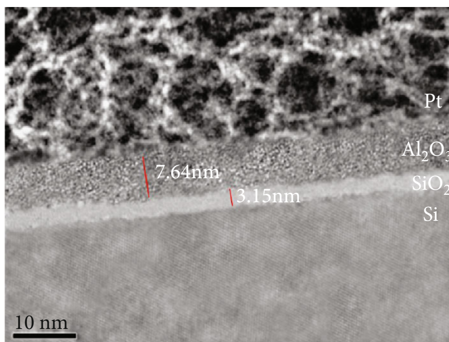

FIGURE 3: TEM picture of $Al_2O_3/SiO_2/Si$ stack after the aluminum oxide was annealed at 600°C for 90 seconds.

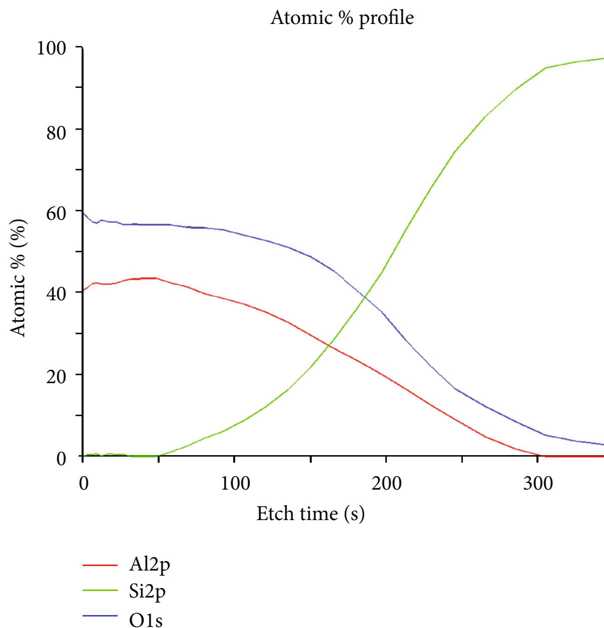

FIGURE 4: XPS measurement of elements near the surface of an annealed sample with ozone-treated Al_2O_3.

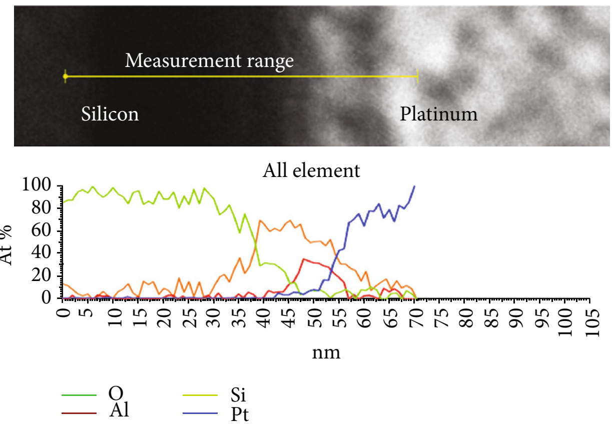

FIGURE 5: EDS analysis for a sample with the stack of $Al_2O_3/SiO_2/Si$ after annealed at 600°C for 90 seconds.

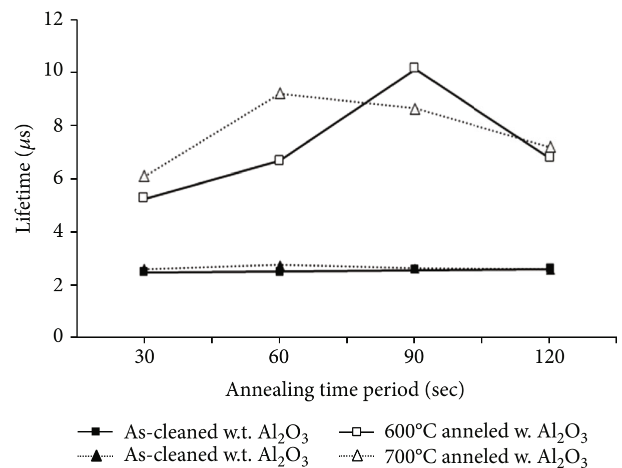

FIGURE 6: Lifetimes of bare wafers achieved at 600°C and 700°C for various annealing time periods. A maximum lifetime of 10.15 μs occurred at 600°C for 90 seconds.

3. Experimental Results

3.1. Lifetime Measurement. First, we measured the lifetimes of bare wafers without Al_2O_3 formed yet on both the front and the rear sides. Figure 6 shows the lifetime measurement results by using the quasi-steady-state photoconductance technique with Sinton WCT-120, at the minority carrier density 10^{15} cm^{-3}. The bare wafers in the dimensions of 5.2×5.2 cm^2 were cleaned by supersonic acetone and were then SC-1 cleaned, followed by a saw damage removal process with a mixture of $CH_3COOH/HF/HNO_3$. Lifetimes of these wafers

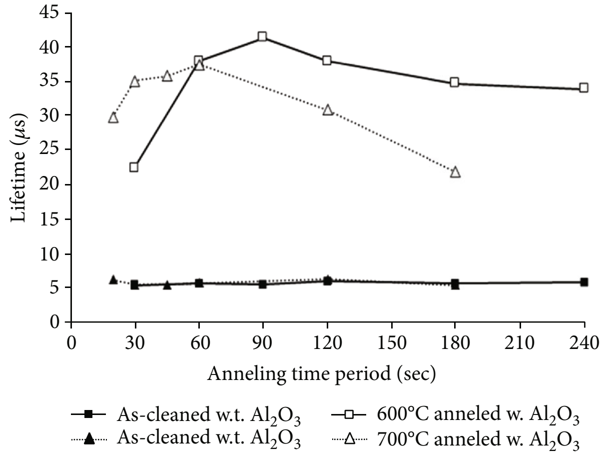

Figure 7: Lifetimes of commercial blue wafers achieved at 600°C and 700°C for various annealing time periods. A maximum lifetime of 41.15 μs occurred at 600°C for 90 seconds.

were measured and then were measured again after Al_2O_3 layers were formed by the ozonation method on both the front and the rear sides. Figure 6 shows the lifetimes for these ozone-treated bare wafers annealed at 600°C (blank squares) and 700°C (blank triangles), respectively, for various annealing time periods. The filled squares and filled triangles in the figure represent the lifetimes of the as-cleaned wafers that were not annealed and were measured here for reference only. The as-annealed wafers with Al_2O_3 layers marked by the blank squares and blank triangles should be compared with the as-cleaned wafers marked by the filled squares and filled triangles, respectively. It can be seen that the lifetime of the ozone-treated wafer annealed at the temperature of 600°C for an annealing time period of 90 seconds could improve by 3.9 times (from 2.6 μs to 10.15 μs) with respect to that of the corresponding as-cleaned wafer. On the other hand, the lifetime improvement for 700°C annealed ozone-treated wafer was 3.3 times at maximum (for an annealing time period of 60 seconds) with respect to that of the corresponding as-cleaned wafer. We have also measured the lifetimes of commercial blue wafers with and without an Al_2O_3 layer on the rear side. Figure 7 shows the lifetimes measured at 600°C and 700°C, respectively, for various annealing time periods. Again, we can see that the time period of 90 seconds was the best annealing time period for 600°C annealing, while the time period of 60 seconds was the best annealing time period for 700°C annealing, and that 600°C annealing supported a better lifetime than 700°C annealing. Likewise, the as-annealed wafers with Al_2O_3 layers are marked by the blank squares (for 600°C annealing) and blank triangles (for 700°C annealing), while the commercial blue wafers without Al_2O_3 layers (denoted by as-cleaned blue wafers) are marked by the filled squares and filled triangles, respectively. These as-cleaned blue wafers were not annealed and are shown only for comparison with the as-annealed blue wafers. The as-annealed blue wafers with Al_2O_3 layers marked by the blank squares and blank triangles should be compared with the as-cleaned blue wafers marked by the filled squares and filled triangles, respectively.

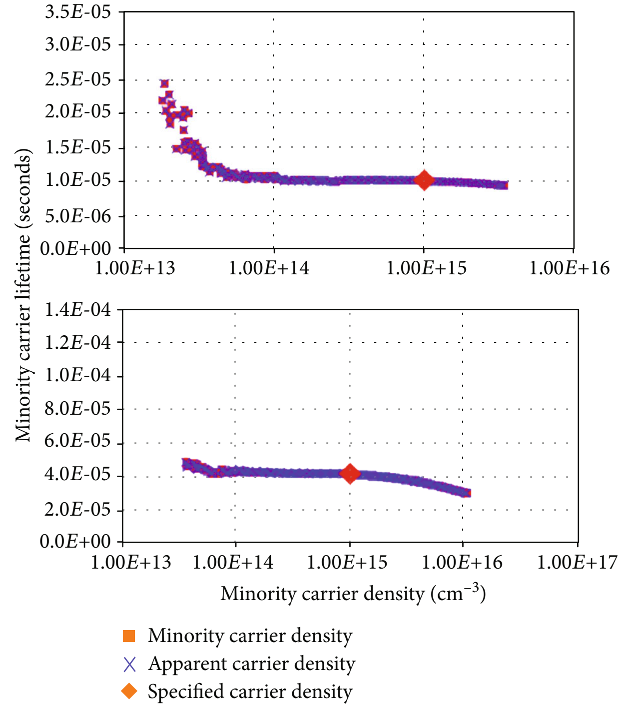

Figure 8: Minority carrier lifetime versus minority carrier density for the ozone-treated bare wafer (top) and the ozone-treated commercial blue wafer (bottom) both annealed at 600°C for 90 seconds. The specified carrier density is 10^{15} cm^{-3}.

Also, we can be aware that the lifetime was improved by 7.3 times (from 5.62 μs to 41.15 μs) at the best annealing condition with respect to the case of no passivation layer on the rear side. Therefore, we adopted 600°C/90 seconds for the annealing condition for the PERC cell fabrication in this study. The density of the negative charges induced by the annealed Al_2O_3 layer was measured by a CV measurement to be -2.30×10^{12} cm^{-2} in the best annealing condition. Figure 8 shows the lifetime versus minority carrier density for the ozone-treated bare wafer (top) and the ozone-treated commercial blue wafer (bottom) both annealed at 600°C for 90 seconds.

3.2. Cell Fabrication. The wafers used for PERC cell fabrication in the study were textured to have caves with inward inclined faces on two sides of the wafers. The sizes of these caves ranged from 1.5 to 3.5 μm, as can be seen from Figure 2. We also measured the lifetimes of these textured wafers with two-side ozone-treated Al_2O_3 layers. Figure 9 shows the lifetimes of the textured wafers with two-side Al_2O_3 layers formed on them and annealed at 600°C for various annealing time periods. The as-cleaned wafers without Al_2O_3 layers were of a textured type but not annealed, and their lifetimes are shown just for comparison with the lifetimes of the textured wafers with two-side ozone-treated Al_2O_3 layers. It can be seen that the best annealing condition for this type of wafers was the same as for standard bare wafers shown previously in Figure 6. Here, the highest lifetime of 10.1 μs occurred in the case of the 90-second annealing time period, which was 4.1 times higher compared to the

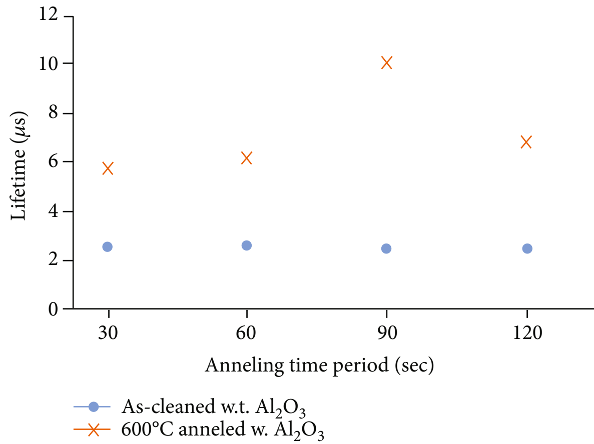

Figure 9: Lifetimes of textured wafers annealed at 600°C for various annealing time periods.

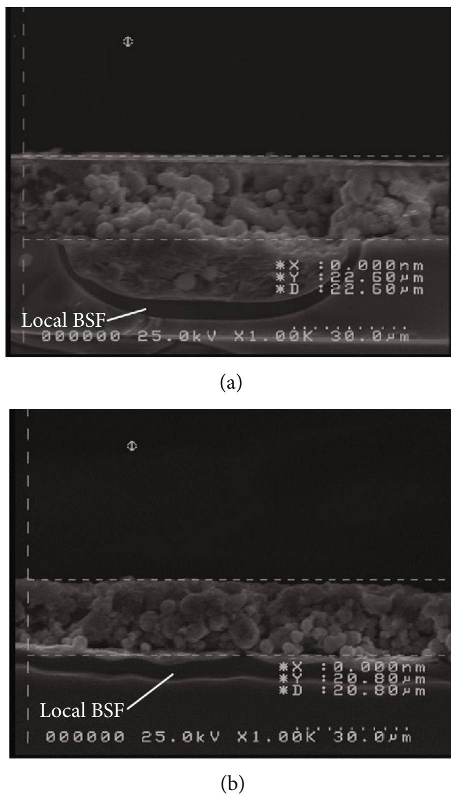

Figure 10: Local BSF for a PERC cell (a) and a full BSF for an Al-BSF cell (b).

case when the wafer was not coated with two-side Al_2O_3 layers.

Then, the textured wafers were used for the fabrication of solar cells. After phosphorus diffused with phosphorus pentoxide wafers used in a tube-based furnace at 870°C, these wafers exhibited a sheet resistance of 80 to 85 Ω/□. Then, the rear sides of the diffused wafers were dipped into a dilute NaOH solution to polish the back surface while the PSG remained on the front surface. The PSG was removed afterward by dipping the wafers into a solution of dilute HF. An Al_2O_3 layer was then coated on the rear side of each wafer using the aforementioned ozonation method, followed by deposition of a PECVD SiNx capping layer of 100 nm thickness on the Al_2O_3 layer. Then, a photolithographic process applied to form a line-shaped pattern of openings by using a H_3PO_4 solution to etch away a part of the SiNx capping layer at 100°C, followed by etching with a HF/HNO_3 solution to form line trenches with a depth of ~30 μm and a width of ~50 μm. Note that the center-to-center spacing between two adjacent line trenches was 1200 μm, and therefore, the coverage for the capping layer was ~96%. At this step, most of the SiNx layer remained and was covered with a photoresist. After the photoresist was removed by acetone, a PECVD SiNx ARC layer of 100 nm thickness was deposited on the front side. Then, the aluminum paste was screen printed on the full surface of the rear side, and the silver paste in a grid

Table 1: Electric parameters and conversion efficiencies measured for Al-BSF cells (A1 and A2) and PERC cells (B1, B2, and B3).

Cell	Jsc (mA/cm^2)	Voc (mV)	F.F. (%)	η (%)
A1	37.32	570	76.7	16.32
A2	37.37	570	76.4	16.27
B1	37.89	590	75.7	16.92
B2	38.14	590	74.7	16.81
B3	37.5	600	75.1	16.73

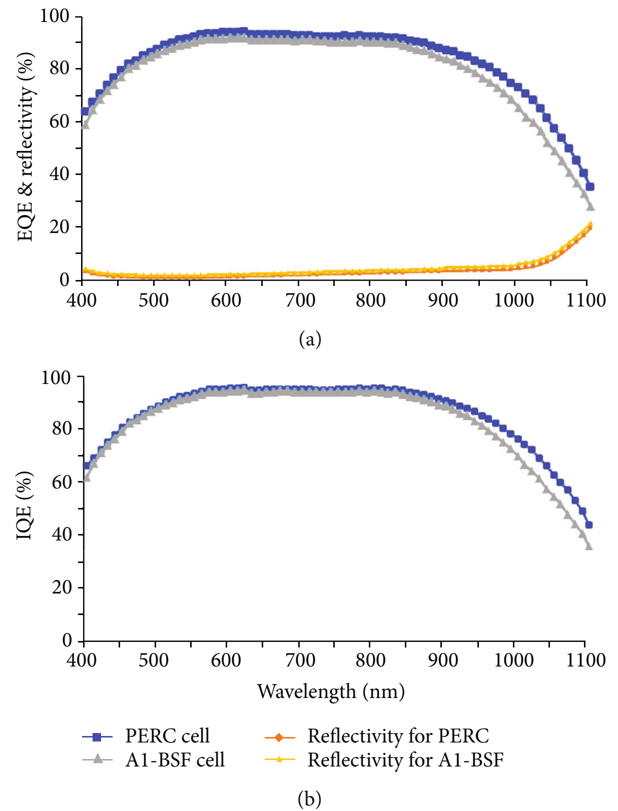

Figure 11: EQE, reflectivity (a), and IQE (b) of the two best cells in this study.

pattern with only one busbar at the center was screen printed on the front side. The widths of the busbar and the fingers were 2 mm and 100 μm, respectively, with the finger spacing being 1.9 mm (edge to edge). After cofired through a conveyor belt furnace, the cells were cut into pieces with the dimensions of $2 \times 2\,cm^2$.

To fabricate conventional cells having the aluminum paste screen-printed on the rear side without a passivation layer (denoted by Al-BSF cells), we followed the previous cell fabrication process except that there were no Al_2O_3/SiNx stack and photolithography required. The resultant back surface fields (BSFs) for PERC cells and Al-BSF cells are, respectively, shown in (a) and (b) of Figure 10.

The cell performances for PERC cells and Al-BSF cells are compared in Table 1. Two cells, A1 and A2, were of Al-BSF type, and three cells, B1~B3, were of PERC type. It can be seen that PERC cells had a better cell efficiency than Al-BSF cells, owing to the fact that a larger short-circuit current and a higher open-circuit voltage could be reached for PERC cells although with a lower fill factor (F.F.). The best PERC cell here had a conversion efficiency of 16.92, which was 0.6% (absolute) higher with respect to the best Al-BSF cell. The external and internal quantum efficiencies (EQE and IQE) of the two best cells are shown in Figure 11, where the front-surface reflectivities for both wafers are also shown. It can be seen that both EQE and IQE are higher for the PERC cell than those for the Al-BSF cell, especially at long wavelengths (e.g., longer than 950 nm).

4. Conclusion

We have presented an ozonation method for forming a passivation layer, i.e., an Al_2O_3 layer on the rear side of a crystalline silicon solar cell. In this method, an aluminum metal film was first deposited and then was oxidized into an Al_2O_3 layer by ozone gas. Lifetimes of the single-crystalline silicon wafers with an ozone-treated Al_2O_3 layer showed ~4 times improvement for bare wafers and 7.3 times improvement for commercial blue wafers. The PERC cells fabricated using textured wafers with such passivation layers showed better conversion efficiency than Al-BSF cells. The best PERC cell showed an efficiency improvement by 0.6% absolute with respect to the best Al-BSF cell in this study.

Data Availability

The raw/processed data for these findings cannot be shared at this time as the data also form part of an ongoing study.

Conflicts of Interest

The authors declare that there is no conflict of interest regarding the publication of this paper.

Acknowledgments

This research was financially supported by the grant 107-2221-E-007-051 from the Ministry of Science and Technology, R.O.C.

References

[1] G. Sebastian, D. Thorsten, and B. Rolf, "Evaluation of series resistance losses in screen-printed solar cells with local rear contacts," *IEEE Journal of Photovoltaics*, vol. 1, no. 1, pp. 37–42, 2011.

[2] V. Naumann, M. Otto, R. B. Wehrspohn, and C. Hagendorf, "Chemical and structural study of electrically passivating Al2O3/Si interfaces prepared by atomic layer deposition," *Journal of Vacuum Science & Technology A: Vacuum, Surfaces, and Films*, vol. 30, no. 4, article 04D106, 2012.

[3] P. Saint-Cast, M. Hofmann, S. Kühnhold et al., "A Review of PECVD aluminium oxide for surface passivation," in *27th European Photovoltaic Solar Energy Conference and Exhibition*, pp. 1797–1801, Frankfurt, Germany, 2012.

[4] J. A. Töfflinger, A. Laades, C. Leendertz et al., "PECVD-AlO_x/-SiN_x passivation stacks on silicon: effective charge dynamics and interface defect state spectroscopy," *Energy Procedia*, vol. 55, pp. 845–854, 2014.

[5] D. Pysch, C. Schmitt, B. Latzel et al., "Implementation of an ALD-Al2O3 PERC-technology into a multi- and monocrystalline industrial pilot production," in *Proceedings of the 29th European Photovoltaic Solar Energy Conference*, pp. 612–616, Amsterdam, Netherlands, 2014.

[6] J. Sheng, J.-H. Lee, W.-H. Choi, T. H. Hong, M. J. Kim, and J.-S. Park, "Review Article: Atomic layer deposition for oxide semiconductor thin film transistors: advances in research and development," *Journal of Vacuum Science & Technology A*, vol. 36, no. 6, article 060801, 2018.

[7] K. Kimoto, Y. Matsui, T. Nabatame et al., "Coordination and interface analysis of atomic-layer-deposition Al2O3 on Si (001) using energy-loss near-edge structures," *Applied physics letters*, vol. 83, no. 21, pp. 4306–4308, 2003.

[8] F. Werner and J. Schmidt, "Manipulating the negative fixed charge density at the c-Si/Al2O3interface," *Applied physics letters*, vol. 104, no. 9, article 091604, 2014.

[9] J. Schmidt, F. Werner, B. Veith et al., "Industrially relevant Al2O3 deposition techniques for the surface passivation of Si solar cells," in *5th World Conference on Photovoltaic Energy Conversion*, Valencia, Spain, 2010.

[10] F. Ye, W. Deng, W. Guo et al., "22.13% efficient industrial p-type mono PERC solar cell," in *IEEE 43rd Photovoltaic Specialists Conference (PVSC)*, Portland, USA, 2016.

[11] G. Krugel, W. Wolke, F. Wagner, J. Rentsch, and R. Preu, "Sputtered aluminum oxide for rear side passivation of p-type silicon solar cells," in *27th European PV Solar Energy Conference and Exhibition*, Frankfurt, Germany, 2012.

[12] Y.-S. Lin, J.-Y. Hung, T.-C. Chen et al., "Effect of post deposition annealing of printed AlOx film on PERC solar cells," in *IEEE 40th Photovoltaic Specialists Conference*, Colorado, U.S.A., 2014.

[13] H.-Q. Xiao, C.-L. Zhou, X.-N. Cao et al., "Excellent passivation of p-type Si surface by sol-gel Al_2O_3 films," *Chinese Physics Letters*, vol. 26, no. 8, article 088102, 2009.

[14] T. Hiramatsu, H. Orita, T. Shirahata, T. Kawaharamura, and S. Fujita, *Solar cell manufacturing method*, 2016, US patent, US 2016/0204301 A1.